



## Strange molecular partners of $P_c$ states in the $\gamma p \rightarrow \phi p$ reaction

Shu-Ming Wu <sup>1,2,\*</sup> Fei Wang,<sup>1,2,†</sup> and Bing-Song Zou <sup>1,2,3,‡</sup>

<sup>1</sup>CAS Key Laboratory of Theoretical Physics, Institute of Theoretical Physics, Chinese Academy of Sciences, Beijing 100190, China

<sup>2</sup>School of Physical Sciences, University of Chinese Academy of Sciences, Beijing 100049, China

<sup>3</sup>School of Physics, Peking University, Beijing 100871, China



(Received 4 July 2023; accepted 27 September 2023; published 11 October 2023)

Based on the high-statistics data of the CLAS Collaboration on the  $\gamma p \rightarrow \phi p$  reaction in the center-of-mass energy range of 2.2 GeV to 2.8 GeV, we investigate the possible existence of strange molecular partners of  $P_c$  states, i.e.,  $N^*(2080)$  and  $N^*(2270)$  as  $K^*\Sigma$  and  $K^*\Sigma^*$  molecular states. In addition to the  $t$ -channel Pomeron exchange,  $t$ -channel meson exchange including pseudoscalar meson ( $\pi$ ,  $\eta$ ), scalar meson [ $\sigma$ ,  $a_0(980)$ ,  $f_0(980)$ ], axial-vector meson  $f_1(1285)$ , tensor meson  $f_2(1270)$ , as well as  $s$ - and  $u$ -channel proton exchange, the inclusion of the  $s$ -channel  $N^*(2080)$  and  $N^*(2270)$  states can fit the data very well. The fitted coupling constants of these  $N^*$  molecular states to  $\phi p$  and  $\gamma p$  are consistent with the results calculated directly from the relevant hadronic triangle diagrams of the hadronic molecular picture.

DOI: [10.1103/PhysRevC.108.045201](https://doi.org/10.1103/PhysRevC.108.045201)

### I. INTRODUCTION

The observation of three narrow  $P_c$  states decaying to  $J/\psi p$  by the LHCb experiment [1,2] has triggered great interests and a lot of efforts to understand their nature [3–5]. In fact, the observed three narrow  $P_c$  states, i.e.,  $P_c(4312)$ ,  $P_c(4440)$ , and  $P_c(4457)$ , are consistent with earlier predictions [6–9] of one narrow  $\bar{D}\Sigma_c$  bound state with spin-parity  $J^P = \frac{1}{2}^-$  and two nearly degenerate narrow  $\bar{D}^*\Sigma_c$  bound states with  $J^P = \frac{1}{2}^-$  &  $\frac{3}{2}^-$ . From heavy quark spin symmetry, one  $\bar{D}\Sigma_c^*$  bound state with  $J^P = \frac{3}{2}^-$  and three  $\bar{D}^*\Sigma_c^*$  bound states with  $J^P = \frac{1}{2}^-$ ,  $\frac{3}{2}^-$  &  $\frac{5}{2}^-$  are also expected to exist [10–12]. Evidence of a  $P_c(4380)$  was claimed by Refs. [1,12], with its mass consistent with the expectation of the  $\bar{D}\Sigma_c^*$  bound state. Since these hidden-charm  $P_c$  states can be successfully and naturally described within the hadronic molecular picture, their strange partners are also expected to exist [13–16]. As the  $P_c$  states were observed through their  $J/\psi p$  decay mode, for those of their strange partners above  $\phi p$  threshold, they are expected to show up in the corresponding  $\phi p$  decay mode. This prompts us to look for the  $K^*\Sigma$  and  $K^*\Sigma^*$  bound states in  $\gamma p \rightarrow \phi p$  reaction.

In 2014, the CLAS Collaboration at Jefferson Laboratory reported high-statistics measurements of differential cross

sections for the reaction  $\gamma p \rightarrow \phi p$  [17,18]. The experimental results show that there may be some structures near the center-of-mass energies  $W = 2.1$  GeV and 2.3 GeV. And there is a bump structure at the forward angle around  $W = 2.1$  GeV.

Before the results of this experiment were released, there were many studies on this process [19–26]. Due to the insufficient statistics of the previous experimental data, the previous models need to be improved accordingly when describing the latest experimental results.

Then based on the latest CLAS data, Yu *et al.* [27] used Reggeized parametrized meson ( $\pi$ ,  $\sigma$ ,  $f_2$ ) exchange and Pomeron exchange to explain this forward angle behavior.

Kim and his collaborators [28,29] considered  $t$ -channel Pomeron exchanges,  $t$ -channel meson exchanges including [ $\pi$ ,  $\eta$ ,  $a_0$ ,  $f_0$ ,  $f_1(1285)$ ],  $s$ -channel and  $u$ -channel proton exchange, and  $s$ -channel nucleon resonances exchange including [ $N^*(2000, 5/2^+)$ ,  $N^*(2300, 1/2^+)$ ] by the Particle Data Group (PDG) [30]. In later work [31], they also considered the  $\phi N \rightarrow \phi N$  final state interaction including the gluon-exchange interaction, the direct  $\phi N$  coupling term, and coupled-channel effects arising from the one-meson-exchange mechanisms in  $\phi N \rightarrow K\Lambda$ ,  $K\Sigma$ ,  $\pi N$ ,  $\rho N$  processes, and found that the effect of the final state interaction of  $\gamma p \rightarrow \phi p$  is very small.

In the  $W = 2.1$ –2.3 GeV energy region for the  $\gamma p \rightarrow \phi p$  reaction, there may be two hadronic molecular states:  $S$ -wave  $K^*\Sigma$  molecule  $N^*(2080)$  and  $S$ -wave  $K^*\Sigma^*$  molecule  $N^*(2270)$ , we examine whether the data can be fitted by using  $N^*(2080)$  and  $N^*(2270)$  instead of previous  $N^*(2000, 5/2^+)$  and  $N^*(2300, 1/2^+)$  for the  $s$ -channel  $N^*$  exchange together with the above-mentioned background terms.

The article is organized as follows. In Sec. II, we present the theoretical framework of our calculation. Our results as well as discussions and a brief summary are shown in Sec. III. The Appendix is presented last.

\*wushuming@mail.itp.ac.cn

†wangfei@mails.ucas.ac.cn

‡zoubs@mail.itp.ac.cn

Published by the American Physical Society under the terms of the [Creative Commons Attribution 4.0 International](https://creativecommons.org/licenses/by/4.0/) license. Further distribution of this work must maintain attribution to the author(s) and the published article's title, journal citation, and DOI. Funded by SCOAP<sup>3</sup>.

## II. THEORETICAL FRAMEWORK

For the reaction of  $\phi$  photoproduction:  $\gamma(k_1) + p(p_1) \rightarrow \phi(k_2) + p(p_2)$  in the center-of-mass system, the four-momenta of these particles can be defined as

$$k_1 = (k, \vec{k}), \quad (1)$$

$$p_1 = (E_p(k), -\vec{k}), \quad (2)$$

$$k_2 = (E_\phi(k'), \vec{k}'), \quad (3)$$

$$p_2 = (E_p(k'), -\vec{k}'), \quad (4)$$

$$P = k_1 + p_1 = k_2 + p_2 = (W, \vec{0}), \quad (5)$$

where  $k(k')$  is the magnitude of three-momenta  $\vec{k}(\vec{k}')$ ,  $E_a(k) = \sqrt{M_a^2 + k^2}$  is the energy of a particle with mass  $M_a$ , and  $W$  is the invariant mass of the system.

Then the differential cross section can be expressed as follows:

$$\frac{d\sigma}{d\Omega} = \frac{1}{64\pi^2 W^2} \frac{k'}{k} \frac{1}{4} \sum_{\text{all spins}} |M_{\lambda_1, s_2, \lambda_2, s_2}(k_1, p_1, k_2, p_2)|^2, \quad (6)$$

where the invariant amplitude  $M$  can be written as

$$\begin{aligned} M_{\lambda_1, s_2, \lambda_2, s_2}(k_1, p_1, k_2, p_2) \\ = \epsilon_\nu^*(k_2, \lambda_2) \bar{u}(p_2, s_2) \mathcal{M}^{\mu\nu}(k_1, p_1, k_2, p_2) \\ \times u(p_1, s_1) \epsilon_\mu(k_1, \lambda_1), \end{aligned} \quad (7)$$

where  $\epsilon_\mu(k_1, \lambda_1)$  and  $\epsilon_\nu^*(k_2, \lambda_2)$  are the polarization vector of photon  $\gamma$  and meson  $\phi$ , respectively,  $u(p_1, s_1)$  and  $\bar{u}(p_2, s_2)$  are the spinor of the incoming and outgoing baryon, respectively, with the normalization  $\bar{u}(p, s)u(p, s') = 2M_p \delta_{s, s'}$ .

As shown in Fig. 1, the full amplitude in our model consists of  $t$ -channel Pomeron exchange,  $t$ -channel meson exchange including pseudoscalar meson ( $\pi, \eta$ ), scalar meson [ $\sigma, a_0(980), f_0(980)$ ], axial-vector meson [ $f_1(1285)$ ], tensor meson [ $f_2(1270)$ ],  $s$ - and  $u$ -channel proton exchange, and  $s$ -channel  $N^*$  molecule exchange. Then,  $\mathcal{M}^{\mu\nu}$  can be written as

$$\mathcal{M}^{\mu\nu} = \mathcal{M}_{t\text{-ch}, \mathbb{P}}^{\mu\nu} + \mathcal{M}_{t\text{-ch}, M}^{\mu\nu} + \mathcal{M}_N^{\mu\nu} + \mathcal{M}_{s\text{-ch}, N^*}^{\mu\nu}. \quad (8)$$

In the following parts, these amplitudes are presented in details.

### A. Pomeron exchange

The Pomeron exchange, based on the Regge phenomenology, stands out as one of the most successful frameworks for describing high-energy elastic scattering. In the study of Donnachie and Landshoff [32], Pomeron is often approximated as a particle with  $I(J^C) = 0(1^+)$ , which primarily couples to the quarks in hadrons. This is shown schematically in Fig. 2. And the Pomeron couples to quarks with  $\gamma_\mu$  type, similar to a photon.

After considering some approximations [19,33,34], the amplitude for Pomeron exchange can be expressed as follows:

$$\mathcal{M}_{t\text{-ch}, \mathbb{P}}^{\mu\nu}(k_1, p_1, k_2, p_2) = G_{\mathbb{P}}(s, t) \mathcal{T}_{\mathbb{P}}^{\mu\nu}(k_1, p_1, k_2, p_2) \quad (9)$$

with  $s = P^2 = W^2$ ,  $t = (p_1 - p_2)^2 = (k_1 - k_2)^2$ ,

$$\begin{aligned} \mathcal{T}_{\mathbb{P}}^{\mu\nu}(k_1, p_1, k_2, p_2) \\ = i12 \frac{eM_\phi^2}{f_\phi} \beta_s F_\phi(t) \beta_{u/d} F_1(t) (\not{k}_1 g^{\mu\nu} - k_1^\nu \gamma^\mu), \end{aligned} \quad (10)$$

where the decay constant  $f_\phi = 13.48$  can be calculated from the decay width of  $\phi \rightarrow e^+ e^-$  in the vector meson dominance (VMD) model [9]. And  $\beta_s$  ( $\beta_{u/d}$ ) is the coupling constant of the Pomeron with the quarks  $s$  ( $u$  or  $d$ ) in the vector meson  $\phi$  (proton  $p$ ). The  $F_\phi(t)$  and  $F_1(t)$  are the form factors for the Pomeron-vector meson vertex and the isoscalar electromagnetic form factor of the nucleon, respectively, which can be expressed as follows:

$$F_\phi(t) = \frac{1}{M_\phi^2 - t} \left( \frac{2\mu_0^2}{2\mu_0^2 + M_\phi^2 - t} \right), \quad (11)$$

$$F_1(t) = \frac{4M_p^2 - 2.8t}{(4M_p^2 - t)(1 - t/0.71 \text{ GeV}^2)^2}, \quad (12)$$

where  $\mu_0$  is a cutoff of the form factor related to the Pomeron-vector meson vertex.

The  $G_{\mathbb{P}}$  in Eq. (9) is the Regge propagator of the Pomeron, and it is written as follows:

$$G_{\mathbb{P}} = \left( \frac{s}{s_0} \right)^{\alpha_P(t)-1} \exp \left\{ -\frac{i\pi}{2} [\alpha_P(t) - 1] \right\} \quad (13)$$

with Regge trajectory  $\alpha_P(t) = \alpha_0 + \alpha'_P t$ .

The parameters  $\mu_0^2, \beta_{u/d}, \beta_s, s_0, \alpha_0, \alpha'_P$  can be determined by fitting the total cross section of  $\rho_0, \omega$ , and  $\phi$  photoproduction at high energies [35]. Here, we use the same values as in Refs. [9,31]:

$$\begin{aligned} \mu_0^2 = 1.1 \text{ GeV}^2, \quad \beta_{u/d} = 2.07 \text{ GeV}^{-1}, \quad \beta_s = 1.386 \text{ GeV}^{-1}, \\ \alpha_0 = 1.08, \quad \alpha'_P = 1/s_0 = 0.25 \text{ GeV}^{-2}. \end{aligned}$$

### B. Meson exchange

In the low-energy region, we also consider  $t$ -channel common meson exchanges, including pseudoscalar meson  $\varphi = \{\pi, \eta\}$ , scalar meson  $S = \{\sigma, a_0(980), f_0(980)\}$ , axial-vector meson  $f_1(1285)$ , and tensor meson  $f_2(1270)$ . The corresponding effective Lagrangians are given as in Refs. [28,31]:

$$\mathcal{L}_{\gamma\varphi\phi} = \frac{e g_{\gamma\varphi\phi}}{M_\phi} \epsilon^{\mu\nu\alpha\beta} \partial_\mu A_\nu \partial_\alpha V_\beta, \quad (14)$$

$$\mathcal{L}_{\gamma S\phi} = \frac{e g_{\gamma S\phi}}{M_\phi} F^{\mu\nu} \phi_{\mu\nu} S, \quad (15)$$

$$\mathcal{L}_{\gamma f_1\phi} = g_{\gamma f_1\phi} \epsilon^{\mu\nu\alpha\beta} \partial_\mu A_\nu \phi_\alpha f_{1\beta}, \quad (16)$$

$$\mathcal{L}_{\gamma f_2\phi} = \frac{g_{\gamma f_2\phi}}{m_0} F_{\mu\alpha} g^{\alpha\beta} \phi_{\beta\nu} f_2^{\mu\nu}, \quad (17)$$

$$\mathcal{L}_{\varphi NN} = -i g_{\varphi NN} \bar{N} \gamma_5 N \varphi, \quad (18)$$

$$\mathcal{L}_{SNN} = g_{SNN} \bar{N} N S, \quad (19)$$

$$\mathcal{L}_{f_1 NN} = -g_{f_1 NN} \bar{N} \gamma_\nu f_1^\mu \gamma_5 N, \quad (20)$$

$$\mathcal{L}_{f_2 NN} = \frac{2g_{f_2 NN}}{M_N} [\bar{N} \gamma_\mu, \partial_\nu] N f_2^{\mu\nu}, \quad (21)$$

where  $\varphi = \{\pi, \eta\}$ ,  $S = \{\sigma, a_0, f_0\}$ ,  $F^{\mu\nu} = \partial^\mu A^\nu - \partial^\nu A^\mu$ ,  $\phi_{\mu\nu} = \partial_\mu \phi_\nu - \partial_\nu \phi_\mu$ .

The amplitudes can be calculated from the above effective Lagrangians:

$$\mathcal{M}_{t\text{-ch},\varphi}^{\mu\nu} = i \frac{eg_\varphi}{M_\phi} \epsilon^{\mu\nu\alpha\beta} k_{1\alpha} k_{2\beta} \gamma_5 \frac{F_\varphi(t)}{t - M_\varphi^2}, \quad (22)$$

$$\mathcal{M}_{t\text{-ch},S}^{\mu\nu} = 2 \frac{eg_S}{M_\phi} (k_1 \cdot k_2 g^{\mu\nu} - k_1^\nu k_2^\mu) \frac{F_S(t)}{t - M_S^2}, \quad (23)$$

$$\mathcal{M}_{t\text{-ch},f_1}^{\mu\nu} = ig_{f_1} \epsilon^{\mu\nu\alpha\beta} \left[ -g_{\alpha\lambda} + \frac{q_{t\alpha} q_{t\lambda}}{M_{f_1}^2} \right] \gamma^\lambda \gamma_5 k_{1\beta} \frac{F_{f_1}(t)}{t - M_{f_1}^2}, \quad (24)$$

$$M_{t\text{-ch},f_2}^{\mu\nu} = \Gamma_{\gamma f_2 \phi}^{\mu\nu\beta\rho} G_{\beta\rho;\lambda\sigma}^2(q_t) \Gamma_{f_2 NN}^{\lambda\sigma} \frac{F_{f_2}(t)}{t - M_{f_2}^2} \quad (25)$$

with  $g_a = g_{\gamma a \phi} g_{a NN}$  ( $a = \{\varphi, S, f_1\}$ ),

$$\Gamma_{\gamma f_2 \phi}^{\mu\nu\beta\rho}(k_1, k_2) = \frac{g_{\gamma f_2 \phi}}{m_0} (k_1^\beta k_2^\rho g^{\mu\nu} + k_1 \cdot k_2 g^{\nu\beta} g^{\mu\rho} - k_1^\nu k_2^\rho g^{\mu\beta} - k_1^\rho k_2^\mu g^{\nu\beta}), \quad (26)$$

$$G_{\beta\rho;\lambda\sigma}^2(q) = \frac{1}{2} (\tilde{g}_{\beta\lambda} \tilde{g}_{\rho\sigma} + \tilde{g}_{\beta\sigma} \tilde{g}_{\lambda\rho}) - \frac{1}{3} \tilde{g}_{\beta\rho} \tilde{g}_{\lambda\sigma}, \quad (27)$$

$$\Gamma_{f_2 NN}^{\lambda\sigma}(p_1, p_2) = \frac{2g_{f_2 NN}}{M_N} (p_1 + p_2)^\lambda \gamma^\sigma \quad (28)$$

with  $m_0 = 1.0$  GeV,  $\tilde{g}^{\beta\rho} = -g^{\beta\rho} + q^\beta q^\rho / m_{f_2}^2$ .  $F_\varphi(t)$ ,  $F_S(t)$ ,  $F_{f_1}(t)$ , and  $F_{f_2}(t)$  are off-shell form factors taken as

$$F_{\varphi,S}(t) = e^{i\beta_{\varphi,S}} \frac{\Lambda_{\varphi,S}^4}{\Lambda_{\varphi,S}^4 + (t - M_{\varphi,S}^2)^2}, \quad (29)$$

$$F_{f_1,f_2}(t) = e^{i\beta_{f_1,f_2}} \left( \frac{\Lambda_{f_1,f_2}^4}{\Lambda_{f_1,f_2}^4 + (t - M_{f_1,f_2}^2)^2} \right)^2. \quad (30)$$

In order to better describe the experiment, we use Regge theory to deal with the  $\sigma$  exchange, the  $f_1$  exchange, and the  $f_2$  exchange, which can be referred to Refs. [27,28]. Then we replace the Feynman propagator  $1/(t - m_\sigma^2)$ ,  $1/(t - m_{f_1}^2)$ , and  $1/(t - m_{f_2}^2)$  with Regge propagator:

$$\begin{aligned} \frac{1}{t - m_\sigma^2} &\rightarrow \mathcal{P}_\sigma(s, t) \\ &= \frac{\pi \alpha'_\sigma \times D_\sigma(t)}{\Gamma[\alpha_\sigma(t) + 1] \sin[\pi \alpha_\sigma(t)]} \times \left( \frac{s}{s_\sigma} \right)^{\alpha_\sigma(t)}, \end{aligned} \quad (31)$$

$$\begin{aligned} \frac{1}{t - m_{f_1}^2} &\rightarrow \mathcal{P}_{f_1}(s, t) \\ &= \frac{\pi \alpha'_{f_1} \times D_{f_1}(t)}{\Gamma[\alpha_{f_1}(t)] \sin[\pi \alpha_{f_1}(t)]} \times \left( \frac{s}{s_{f_1}} \right)^{\alpha_{f_1}(t)-1}, \end{aligned} \quad (32)$$

$$\begin{aligned} \frac{1}{t - m_{f_2}^2} &\rightarrow \mathcal{P}_{f_2}(s, t) \\ &= \frac{\pi \alpha'_{f_2} \times D_{f_2}(t)}{\Gamma[\alpha_{f_2}(t) - 1] \sin[\pi \alpha_{f_2}(t)]} \times \left( \frac{s}{s_{f_2}} \right)^{\alpha_{f_2}(t)-2} \end{aligned} \quad (33)$$

with  $s_\sigma = s_{f_1} = s_{f_2} = 1.0$  GeV<sup>2</sup>. The Regge trajectories  $[\alpha_\sigma(t), \alpha_{f_1}(t), \alpha_{f_2}(t)]$  and phases  $[D_\sigma(t), D_{f_1}(t), D_{f_2}(t)]$  take the following form:

$$\alpha_\sigma(t) = \alpha_\sigma^0 + \alpha'_\sigma t = -0.175 + 0.7 t, \quad (34)$$

$$\alpha_{f_1}(t) = \alpha_{f_1}^0 + \alpha'_{f_1} t = 0.95 + 0.028 t, \quad (35)$$

$$\alpha_{f_2}(t) = \alpha_{f_2}^0 + \alpha'_{f_2} t = 0.537 + 0.9 t, \quad (36)$$

$$D_\sigma(t) = \frac{e^{-i\pi\alpha_\sigma(t)} + 1}{2}, \quad (37)$$

$$D_{f_1}(t) = \frac{e^{-i\pi\alpha_{f_1}(t)} - 1}{2}, \quad (38)$$

$$D_{f_2}(t) = \frac{e^{-i\pi\alpha_{f_2}(t)} + 1}{2}. \quad (39)$$

The coupling constants in Eqs. (14), (15), (16) can be determined by the radiative decays of  $\phi$  and  $f_1$ . Using the branching ratios data in PDG [30],

$$\text{Br}_{\phi \rightarrow \pi^0 \gamma} = (1.32 \pm 0.05) \times 10^{-3},$$

$$\text{Br}_{\phi \rightarrow \eta \gamma} = (1.301 \pm 0.025) \times 10^{-2},$$

$$\text{Br}_{\phi \rightarrow a_0 \gamma} = (7.6 \pm 0.6) \times 10^{-5},$$

$$\text{Br}_{\phi \rightarrow f_0 \gamma} = (3.22 \pm 0.19) \times 10^{-4},$$

$$\text{Br}_{f_1 \rightarrow \gamma \phi} = (7.4 \pm 2.6) \times 10^{-4},$$

we can get the relevant coupling constants

$$g_{\gamma \pi \phi} = -0.14,$$

$$g_{\gamma \eta \phi} = -0.71,$$

$$g_{\gamma a_0 \phi} = -0.77,$$

$$g_{\gamma f_0 \phi} = -2.44,$$

$$g_{\gamma f_1 \phi} = 0.17.$$

The coupling constants in Eqs. (18), (19) can be determined by the Nijmegen potential as

$$g_{\pi NN} = 13.0,$$

$$g_{\eta NN} = 6.34,$$

$$g_{a_0 NN} = 4.95,$$

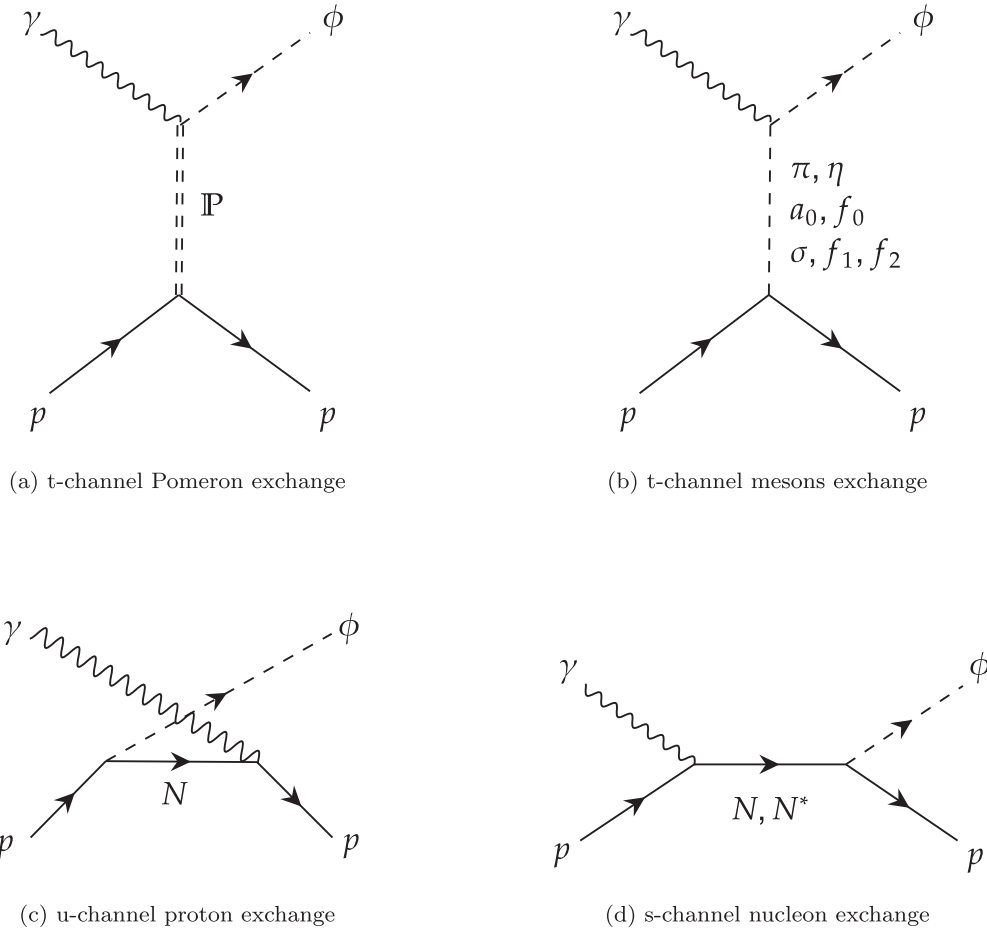
$$g_{f_0 NN} = -0.51.$$

The other coupling constants are considered as fitting parameters within some given ranges. For the  $\sigma$  exchange, the value of  $g_\sigma = g_{\gamma \sigma \phi} g_{\sigma NN}$  falls within the range of 0.5–1.5. The selection of the range can be found in Ref. [27]. For the  $f_1$  exchange, the value of  $g_{f_1 NN}$  can be taken from 2.0 [36] to 5.8 [37]. So, the value of  $g_{f_1} = g_{\gamma f_1 \phi} g_{f_1 NN}$  is within the range of 0.3–1.0. For the  $f_2$  exchange, we take the value of  $g_{f_2} = g_{\gamma f_2 \phi} g_{f_2 NN}$  to be within the range of 0.1–1.0.

The cutoff parameters ( $\Lambda_\varphi, \Lambda_S, \Lambda_\sigma, \Lambda_{f_1}, \Lambda_{f_2}$ ) and the amplitude phases ( $\beta_\varphi, \beta_S, \beta_\sigma, \beta_{f_1}, \beta_{f_2}$ ) are the fitting parameters.

### C. Proton exchange

Considering proton exchange in the  $s$  and  $u$  channels, from the perspective of gauge invariance, the two amplitudes must


 FIG. 1. Relevant Feynman diagrams for  $\gamma p \rightarrow \phi p$ .

be taken together. The associated effective Lagrangians can be written as

$$\mathcal{L}_{\gamma NN} = -e\bar{N}\left(\gamma_\mu - \frac{\kappa_N}{2M_N}\sigma_{\mu\nu}\partial^\nu\right)NA^\mu, \quad (40)$$

$$\mathcal{L}_{\phi NN} = -g_{\phi NN}\bar{N}\left(\gamma_\mu - \frac{\kappa_{\phi NN}}{2M_N}\sigma_{\mu\nu}\partial^\nu\right)N\phi^\mu. \quad (41)$$

And the amplitudes can be written as

$$\mathcal{M}_N^{\mu\nu}(p_1, k_1, p_2, k_2) = (\mathcal{M}_{s-ch,p}^{\mu\nu} + \mathcal{M}_{u-ch,p}^{\mu\nu})F_p(s, u), \quad (42)$$

$$\begin{aligned} \mathcal{M}_{s-ch,p}^{\mu\nu}(p_1, k_1, p_2, k_2) &= \frac{eg_{\phi NN}}{s - M_N^2}\left(\gamma^\nu - i\frac{\kappa_{\phi NN}}{2M_N}\sigma^{\nu\alpha}k_{2\alpha}\right) \\ &\quad \times (\not{q}_s + M_N)\left(\gamma^\mu + i\frac{\kappa_p}{2M_N}\sigma^{\mu\beta}k_{1\beta}\right), \\ \mathcal{M}_{u-ch,p}^{\mu\nu}(p_1, k_1, p_2, k_2) &= \frac{eg_{\phi NN}}{u - M_N^2}\left(\gamma^\mu + i\frac{\kappa_p}{2M_N}\sigma^{\mu\alpha}k_{1\alpha}\right) \\ &\quad \times (\not{q}_u + M_N)\left(\gamma^\nu - i\frac{\kappa_{\phi NN}}{2M_N}\sigma^{\nu\beta}k_{2\beta}\right), \end{aligned} \quad (43)$$

where  $q_s = k_1 + p_1$ ,  $q_u = p_1 - k_2$ ,  $u = q_u^2$ .  $F_p(s, u)$  is a form factor, taken from Ref. [31]:

$$F_p(s, u) = e^{i\beta p} [F_p(s) + F_p(u) - F_p(s)F_p(u)]^2, \quad (44)$$

$$F_p(s) = \frac{\Lambda_p^4}{\Lambda_p^4 + (s - M_p^2)^2},$$

$$F_p(u) = \frac{\Lambda_p^4}{\Lambda_p^4 + (u - M_p^2)^2}. \quad (45)$$

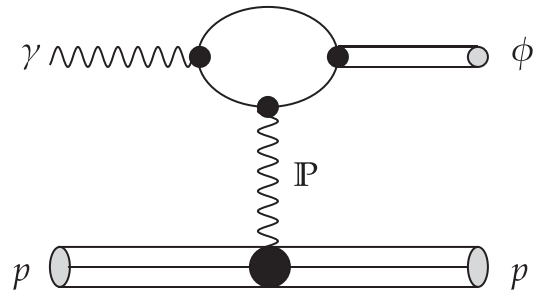

 FIG. 2. The Pomeron exchange mechanism of  $\gamma p \rightarrow \phi p$  in quark level.

TABLE I. The model parameters.

Phases		Cutoffs (GeV)		Other constants			
$\beta_{ps}$	$2.699 \pm 0.027$	$\Lambda_{ps}$	$0.36 \pm 0.07$	$g_\sigma$	$0.540 \pm 0.029$	$\Gamma_{N_2^*}(\text{GeV})$	$0.23 \pm 0.04$
$\beta_s$	$3.255 \pm 0.033$	$\Lambda_s$	$0.751 \pm 0.028$	$g_{f_1}$	$0.86 \pm 0.17$	$g'_1$	$2.5 \pm 0.5$
$\beta_p$	$5.76 \pm 0.06$	$\Lambda_p$	$0.766 \pm 0.021$	$g_{f_2}$	$0.25 \pm 0.04$	$g'_2$	$-2.0 \pm 0.6$
$\beta_\sigma$	$2.830 \pm 0.028$	$\Lambda_\sigma$	$2.00 \pm 0.02$	$\Gamma_{N_1^*}(\text{GeV})$	$0.099 \pm 0.011$	$g'_3$	$2.5 \pm 0.6$
$\beta_{f_1}$	$0.419 \pm 0.004$	$\Lambda_{f_1}$	$1.47 \pm 0.06$	$g_1$	$0.0395 \pm 0.0024$	$h'_2$	$-0.90 \pm 0.05$
$\beta_{f_2}$	$3.027 \pm 0.030$	$\Lambda_{f_2}$	$1.96 \pm 0.15$	$g_2$	$0.095 \pm 0.007$		
$\beta_{N_1^*}$	$2.733 \pm 0.027$	$\Lambda_{N_1^*}$	$1.432 \pm 0.022$	$g_3$	$0.1937 \pm 0.0034$		
$\beta_{N_2^*}$	$1.001 \pm 0.010$	$\Lambda_{N_2^*}$	$0.752 \pm 0.028$	$h_2$	$-9.5 \pm 0.5$		

In this part, the coupling constant  $\kappa_N$  is the anomalous magnetic moment of the nucleon. For the proton,  $\kappa_p = 1.79$ . And  $g_{\phi NN}$ ,  $\kappa_{\phi NN}$  can be determined by the Nijmegen potential model [38,39]. There, we take  $g_{\phi NN} = -1.47$ ,  $\kappa_{\phi NN} = -1.65$  [31]. The cutoff  $\Lambda_p$  and relative phase  $\beta_p$  are fitting parameters.

#### D. $N^*$ molecule exchange

As the  $P_c$  states observed by the LHCb collaboration can be well described by the  $S$ -wave  $\bar{D}\Sigma_c$ ,  $\bar{D}\Sigma_c^*$ , and  $\bar{D}^*\Sigma_c$  molecular states [6,7,40,41] with three  $\bar{D}^*\Sigma_c^*$  bound states with  $J^P = \frac{1}{2}^-$ ,  $\frac{3}{2}^-$ , and  $\frac{5}{2}^-$  expected to exist from heavy quark spin symmetry [10–12], their hidden strange partners are also expected to exist [13,15]. For the process of  $\gamma p \rightarrow \phi p$ , the CLAS data [17,18] observed two peaks around  $K^*\Sigma$  and  $K^*\Sigma^*$  thresholds, respectively. We expect these peaks to be due to  $K^*\Sigma$  and  $K^*\Sigma^*$  molecular states, denoted as  $N^*(2080)$  and  $N^*(2270)$ , respectively. Since the energy range is not far away from the  $p\phi$  threshold, the  $S$  wave is dominant. We consider only  $N^*(2080)(3/2^-)$  [30] and  $N^*(2270)(1/2^- \text{ or } 3/2^-)$ . For the process  $N^* \rightarrow K^*\Sigma^{(*)} \rightarrow \gamma(\phi)N$ , it can be represented by a triangle diagram, as explained in the Appendix in detail. For simplicity, we describe these two processes with tree-level diagrams. The corresponding coupling constants are treated as fitting parameters, which are going to be compared with the results of triangle diagram calculations.

The corresponding effective Lagrangians can be written as [42]

$$\mathcal{L}_{RN\gamma}\left(\frac{1}{2}^\pm\right) = \frac{ef_1}{2M_N} \bar{N} \Gamma^{(\mp)} \sigma_{\mu\nu} \partial^\nu A^\mu R, \quad (46)$$

$$\begin{aligned} \mathcal{L}_{RN\gamma}\left(\frac{3}{2}^\pm\right) &= -\frac{ief_1}{2M_N} \bar{N} \Gamma_v^{(\pm)} F^{\mu\nu} R_\mu \\ &\quad - \frac{ef_2}{(2M_N)^2} \partial_\nu \bar{N} \Gamma^{(\pm)} F^{\mu\nu} R_\mu, \end{aligned} \quad (47)$$

$$\begin{aligned} \mathcal{L}_{RNV}\left(\frac{1}{2}^\pm\right) &= \bar{R} \left[ \pm \frac{g_1 M_V^2}{2M_N(M_R \mp M_N)} \Gamma_\mu^{(\mp)} N \right. \\ &\quad \left. + \frac{g_2}{2M_N} \Gamma^{(\mp)} \sigma_{\mu\nu} N \partial^\nu \right] V^\mu, \\ \mathcal{L}_{RNV}\left(\frac{3}{2}^\pm\right) &= \bar{R}_\mu \left[ \frac{ig_1}{2M_N} \Gamma_v^{(\pm)} N \pm \frac{g_2}{(2M_N)^2} \Gamma^{(\pm)} \partial_\nu N \right. \\ &\quad \left. \mp \frac{g_3}{(2M_N)^2} \Gamma^{(\pm)} N \partial_\nu \right] V^{\mu\nu}, \end{aligned} \quad (48)$$

where  $R$  and  $R_\mu$  are the fields for the spin-1/2 and 3/2 resonances, respectively.  $V$  and  $N$  are the spin-1 vector meson and baryon, respectively. And  $V^{\mu\nu} = \partial^\mu V^\nu - \partial^\nu V^\mu$  with  $\Gamma_\mu^{(\pm)} = \begin{pmatrix} \gamma_\mu \gamma_5 \\ \gamma_\mu \end{pmatrix}$ ,  $\Gamma^{(\pm)} = \begin{pmatrix} \gamma_5 \\ 1 \end{pmatrix}$ .

Then the  $N^*$  exchange amplitudes can be written as

$$\mathcal{M}_{s\text{-}ch,N^*}^{\mu\nu}(1/2^-) = F_R(s) \left( \frac{g_1 M_V^2}{2M_N(M_R \mp M_N)} \gamma_\nu \gamma_5 + \frac{g_2}{2M_N} i\sigma_{\nu\alpha} k_2^\alpha \gamma_5 \right) G^{\frac{1}{2}}(q_s) \frac{ef_1}{2M_N} \gamma_5 (-i) \sigma_{\mu\beta} k_1^\beta, \quad (49)$$

$$\mathcal{M}_{s\text{-}ch,N^*}^{\mu\nu}(3/2^-) = F_R(s) \left( \frac{g_1}{2M_N} \gamma_\rho + \frac{(g_2 p_2 - g_3 k_2)_\rho}{4M_N^2} \right) (k_2^\alpha g^{\rho\mu} - k_2^\rho g^{\alpha\mu}) G_{\alpha\beta}^{\frac{3}{2}}(q_s) \left( \frac{ef_1}{2M_N} \gamma_\sigma + \frac{ef_2}{4M_N^2} (p_1)_\sigma \right) (k_1^\beta g^{\sigma\mu} - k_1^\sigma g^{\beta\mu}), \quad (50)$$

where

$$G^{\frac{1}{2}}(p) = \frac{i(\not{p} + M_R)}{s - M_R^2 + iM_R \Gamma_R}, \quad (51)$$

$$G_{\mu\nu}^{\frac{3}{2}}(p) = \frac{i(\not{p} + M_R)}{s - M_R^2 + iM_R \Gamma_R} \left( -g_{\mu\nu} + \frac{1}{3} \gamma_\mu \gamma_\nu + \frac{2}{3} \frac{p_\mu p_\nu}{M_R^2} + \frac{1}{3M_R} (\gamma_\mu p_\nu - \gamma_\nu p_\mu) \right). \quad (52)$$

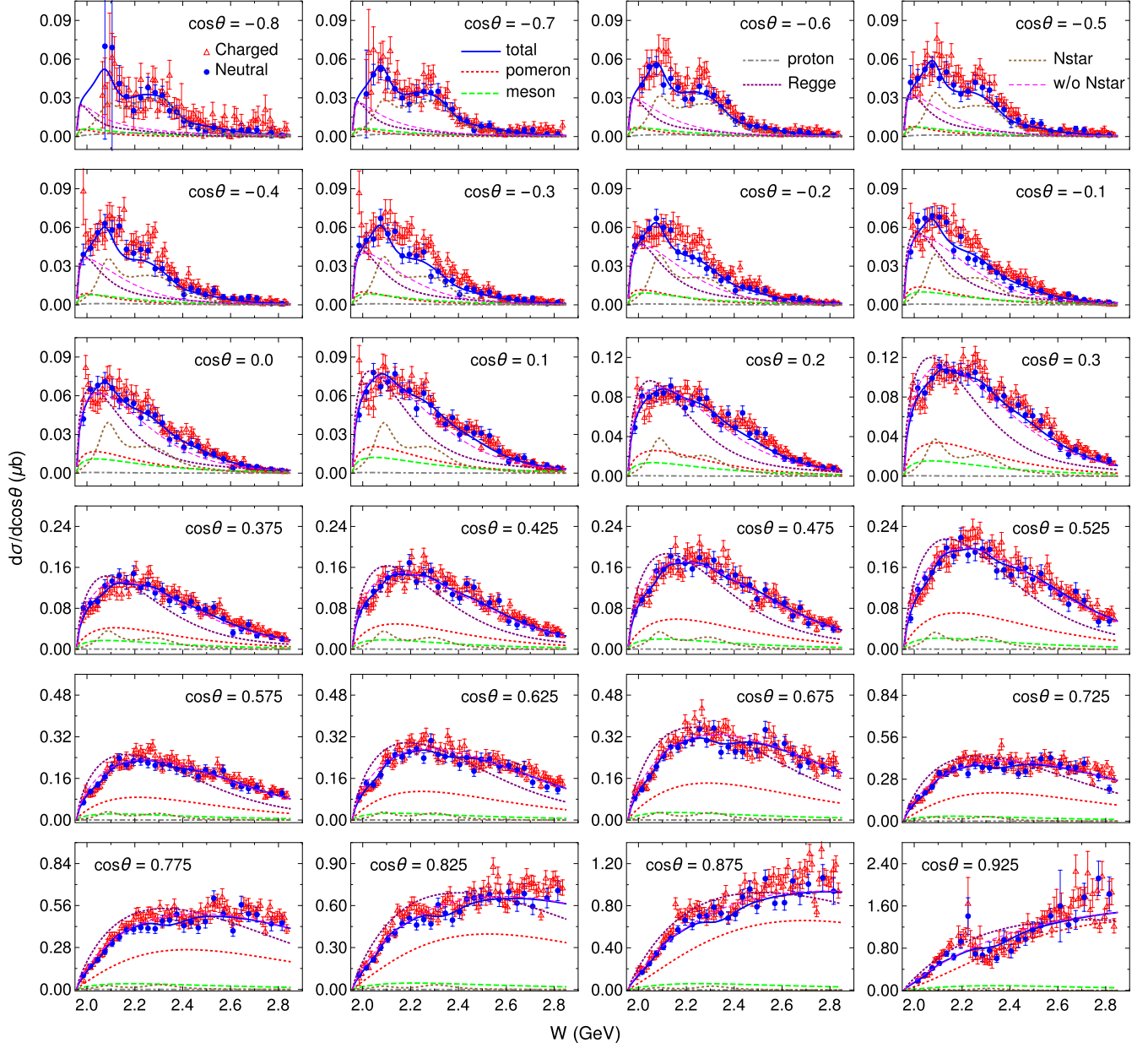


FIG. 3. Differential cross sections  $d\sigma/d\cos\theta(\mu\text{b})$  as a function of  $W(\text{GeV})$  at different  $\cos\theta$ . The blue solid line stands for the total contribution. The red dotted line, green dashed line, gray dash-dotted line, purple dotted line, and brown dotted line correspond to the contributions from Pomeron exchange, pseudoscalar and scalar mesons ( $\pi$ ,  $\eta$ ,  $a_0$ ,  $f_0$ ) exchange,  $s$ - and  $u$ -channel proton exchange, Reggeized mesons ( $\sigma$ ,  $f_1$ ,  $f_2$ ) exchange, and two  $N^*$  molecules exchange, respectively. The magenta dashed line represents the full contribution without the  $N^*$  exchange. The experimental data are taken from Ref. [17], where the red triangles and blue circles represent the charged- and neutral-mode, respectively.

The form factor  $F_R(s)$  takes the following form:

$$F_R(s) = e^{i\beta_R} e^{-\frac{(s-m_R^2)^2}{\Lambda_R^4}}. \quad (53)$$

For  $N^*(2080)$ ,  $J^P = 3/2^-$ , these parameters need to be fitted:

$$h_2(f_2/f_1), g_1, g_2, g_3, \beta_{N_1^*}, \Lambda_{N_1^*}, \Gamma_{N_1^*}.$$

For  $N^*(2270)$ ,  $J^P = 3/2^-(1/2^-)$ , the fitted parameters are

$$h_2'(f_2'/f_1'), g_1', g_2', g_3', \beta_{N_2^*}, \Lambda_{N_2^*}, \Gamma_{N_2^*}, \\ (g_1'/f_1', g_2'/f_1', \beta_{N_2^*}, \Lambda_{N_2^*}, \Gamma_{N_2^*}).$$

### III. RESULTS AND DISCUSSIONS

According to the  $K\bar{K}$  decay mode of the  $\phi$ , the CLAS Collaboration divided the results of  $\gamma p \rightarrow \phi p$

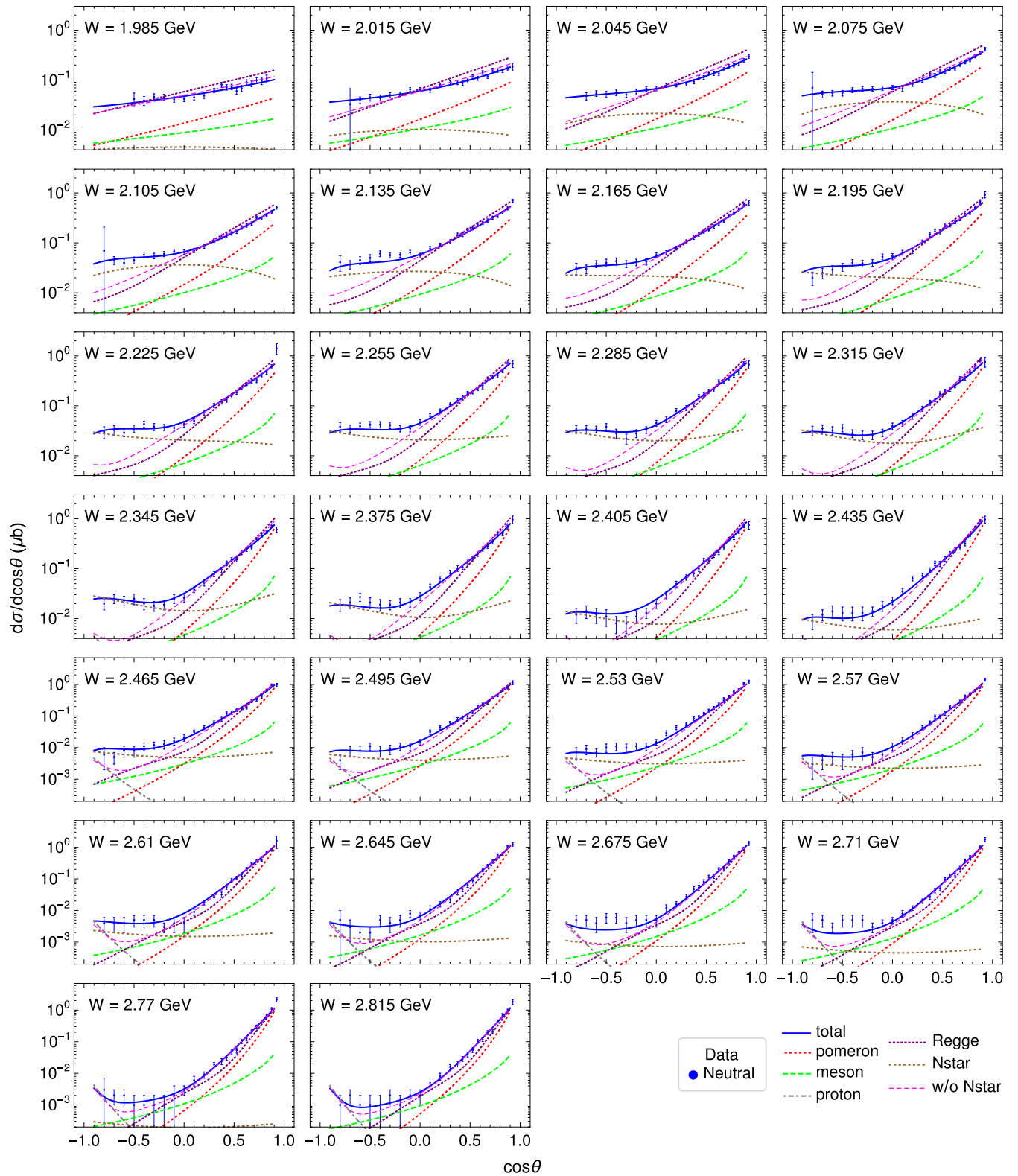


FIG. 4. Differential cross sections  $d\sigma/d\cos\theta$  ( $\mu\text{b}$ ) as a function of  $\cos\theta$  at different  $W$  (GeV). The marks are the same as in Fig. 3.

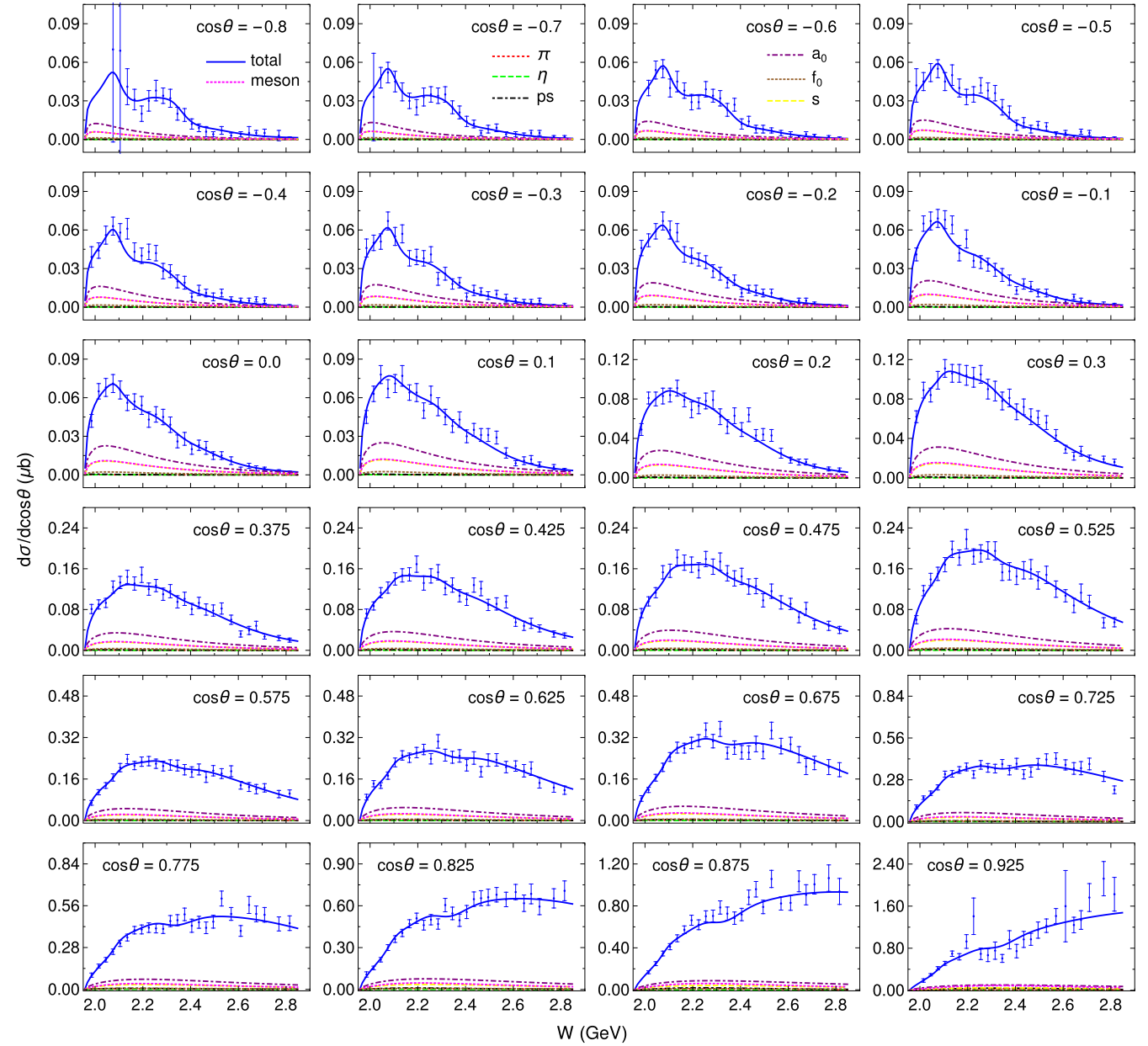


FIG. 5. Mesons contribution to the differential cross sections  $d\sigma/d\cos\theta$  ( $\mu\text{b}$ ) as a function of  $W$  (GeV) at different  $\cos\theta$ .

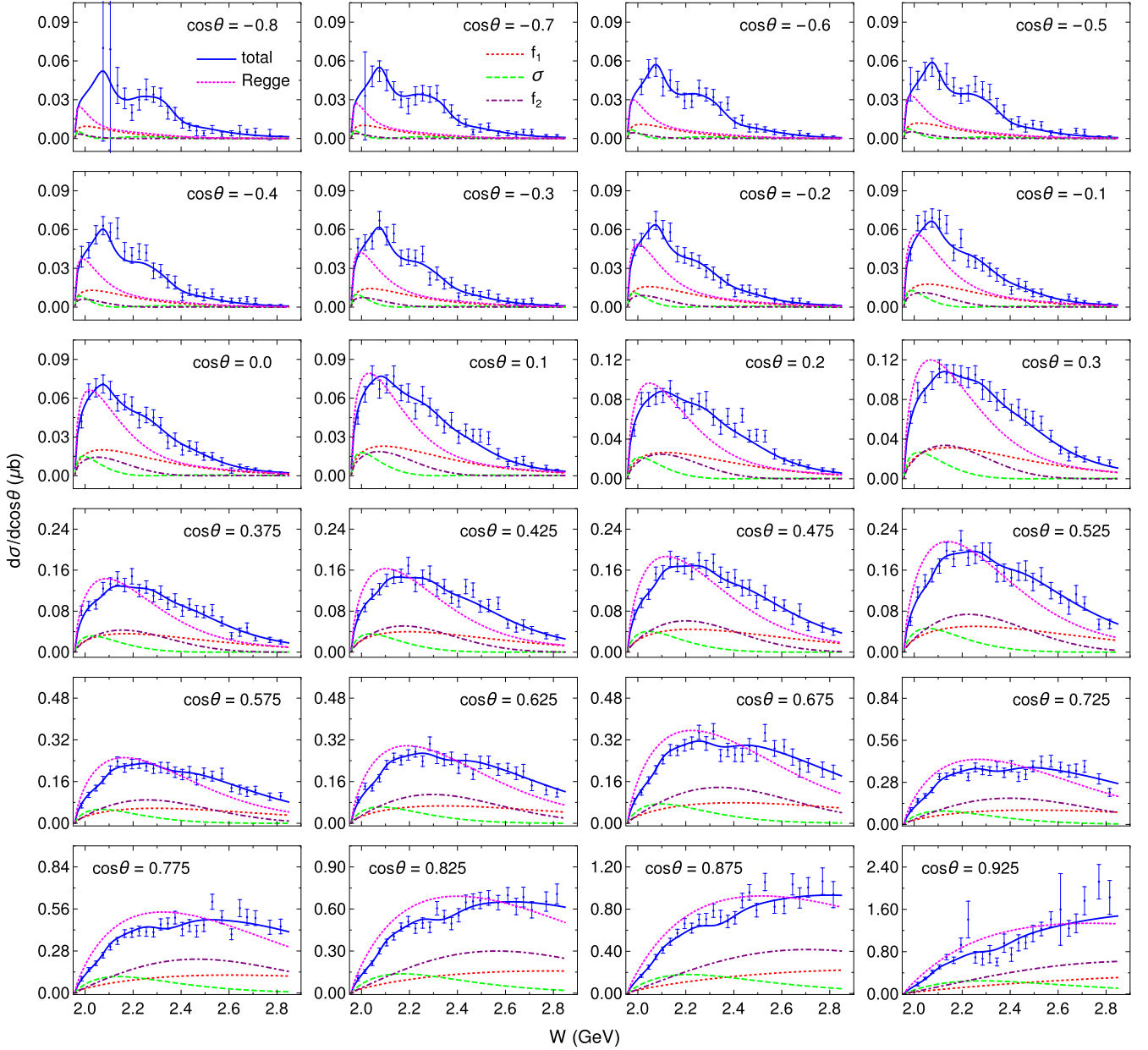
into charged- ( $\phi \rightarrow K^+K^-$ ) and neutral- ( $\phi \rightarrow K_S^0K_L^0$ ) modes. Considering the contamination of the process  $\gamma p \rightarrow K^+\Lambda(1520)/\Lambda(1800) \rightarrow pK^+K^-$  on the charged mode, although relevant cuts have been done in the experiment, we only use the neutral mode to fit.

By using the MINUIT algorithm [43–45] to minimize the  $\chi^2$  function, we fit the experimental data of the differential cross section  $d\sigma/d\cos\theta$  in Eq. (6) and obtain the best fitting result  $\chi^2/\text{dof} = 0.87$ . Since with  $J^P[N^*(2270)] = 1/2^-$ , we cannot get good fitting results, so we only show  $J^P = 3/2^-$  results. The corresponding parameters and results are shown in Table I and Figs. 3–7.

Based on the fitting results, the following observations can be made:

- (i) Proton exchange: The contribution of proton exchange can be negligible in all regions.
- (ii) Pomeron exchange: The contribution of Pomeron exchange is relatively small in the backward angle region. However, as  $\cos\theta$  increases, its contribution starts to increase. It becomes the main contributor to the differential cross section when  $\cos\theta \sim 1$ , and its contribution increases with the center-of-mass energy in this region. In other angles, the contribution of Pomeron exchange tends to increase initially and then decrease.
- (iii) Meson ( $\pi, \eta, a_0, f_0$ ) exchange: The overall contribution of meson exchange to the differential cross section is relatively small. It also increases initially




 FIG. 6. Reggeized mesons contribution to the differential cross sections  $d\sigma/d\cos\theta$  ( $\mu\text{b}$ ) as a function of  $W$  (GeV) at different  $\cos\theta$ .

and then decreases with the center-of-mass energy. Among the mesons, the contribution of pseudoscalar mesons is much smaller than that of scalar mesons, and the contributions of  $\eta$  and  $f_0$  are much smaller than those of  $\pi$  and  $a_0$ , respectively.

- (iv) Reggeized parametrized mesons ( $\sigma$ ,  $f_1$ ,  $f_2$ ) exchange: The contribution of Reggeized parametrized mesons to the differential cross section is minimal in the backward angle region, except near the threshold. Their contribution becomes larger as the angle increases. The change trend with the center-of-mass energy is similar to that of meson exchange with a peak whose position and height increase with the angle.
- (v)  $N^*$  molecules exchange: The contribution of  $N^*$  molecules exchange is most dominant in the backward angle region and smaller in other regions.

Considering the behavior of the total cross section, in the high-energy region, besides the largest contribution from the Pomeron, only the Reggeized parametrized mesons contribute significantly. Due to their relative phase, the exchange of Reggeized mesons has little effect on the total cross section.

From the fitting results about  $N^*$  molecules exchange:

$$\begin{aligned} \Gamma_{N_1^*} &= 0.099 \pm 0.011 \text{ GeV}, & \Gamma_{N_2^*} &= 0.23 \pm 0.04 \text{ GeV}, \\ g_1 &= 0.0395 \pm 0.0024, & g_2 &= 0.095 \pm 0.007, \\ g_3 &= 0.1937 \pm 0.0034, & f_2/f_1 &= -9.5 \pm 0.5, \\ g'_1 &= 2.5 \pm 0.5, & g'_2 &= -2.0 \pm 0.6, \\ g'_3 &= 2.5 \pm 0.6, & f'_2/f'_1 &= -0.90 \pm 0.05, \end{aligned}$$

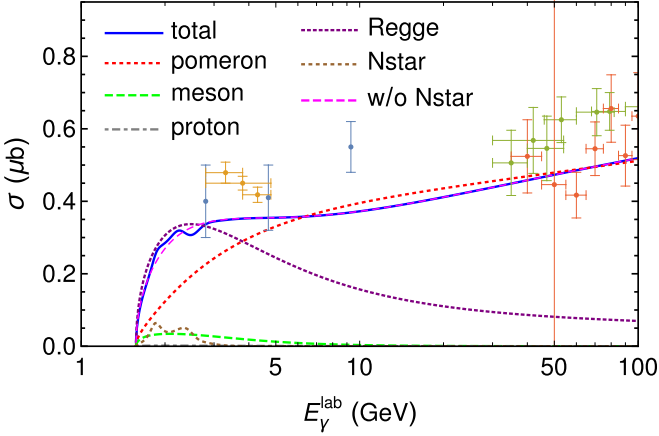


FIG. 7. Total cross section  $\sigma$  ( $\mu\text{b}$ ) as a function of the photon energy in the laboratory frame  $E_\gamma^{\text{lab}}$  (GeV). Experimental data come from Refs. [46–49].

we can calculate the properties

$$A_{3/2}/A_{1/2} = 1.60 \pm 0.13,$$

$$A'_{3/2}/A'_{1/2} = -1.12 \pm 0.25,$$

$$\Gamma_{N_1^* \rightarrow p\phi} \times \Gamma_{N_1^* \rightarrow \gamma p} = (8.2 \pm 2.6) \times 10^{-4} \text{ MeV}^2,$$

$$\Gamma_{N_2^* \rightarrow p\phi} \times \Gamma_{N_2^* \rightarrow \gamma p} = (6 \pm 6) \times 10^{-3} \text{ MeV}^2.$$

The above results are roughly consistent with the calculation from the molecular state triangle diagram in the Appendix at small cutoffs  $\Lambda_0 = 0.6\text{--}0.8$  GeV and  $\Lambda_1 = 0.8\text{--}1.0$  GeV. Then, we discuss other mechanisms that may affect this process.

First, for the charged mode, we need to consider the final state of the three-body decay. The corresponding process is  $\gamma p \rightarrow \phi p$ ,  $K^+\Lambda(1520)$ ,  $K^+\Lambda(1800) \rightarrow pK^+K^-$ . After adding the corresponding hard cuts of  $M_{pK^-}$  according to the experimental analysis, we can simultaneously fit both the charged-mode data and the neutral-mode data.

Second, the thresholds of  $K^+\Lambda(1520)$  and  $p\phi$  are very close. So there may be coupled-channel effects [26]. Then we can fit the experiment data of both  $K^+\Lambda(1520)$  and  $p\phi$  together.

In summary, through fitting the experimental data of CLAS in 2014, we carefully analyzed the process of  $\gamma p \rightarrow \phi p$ . It is found that the data can be fitted well by using  $N^*(2080)$  and  $N^*(2270)$  instead of previous  $N^*(2000, 5/2^+)$

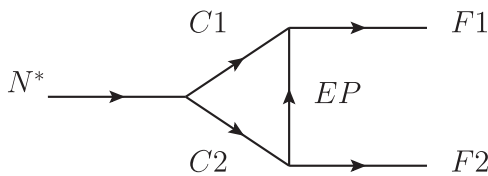


FIG. 8. The triangle diagram for the two-body decays of the exotic  $N^*$ s in the  $K^*\Sigma^*$  and  $K^*\Sigma$  molecular pictures, where  $C1$ ,  $C2$  denote the constituent particles of the composite system  $K^*\Sigma^*$  or  $K^*\Sigma$ ,  $F1$ ,  $F2$  denote the final states,  $EP$  denotes the exchanged particles.

TABLE II. Used decay channels of  $N^*$ .

Initial state	Final states	Exchanged particles
$N^*(2270)(K^*\Sigma^*)$	$p\phi$	$K, K^*$
	$\gamma p$	$K$
$N^*(2080)(K^*\Sigma)$	$p\phi$	$K, K^*$
	$\gamma p$	$K$

and  $N^*(2300, 1/2^+)$  for the  $s$ -channel  $N^*$  exchange together with other background terms. The fitted coupling constants of these  $N^*$  molecular states to  $p\phi$  and  $\gamma p$  are consistent with the results calculated directly from the relevant hadronic triangle diagrams of the molecular picture. The new solution gives a natural explanation of the two  $N^*$  peaks in the process of  $\gamma p \rightarrow \phi p$ , a further support of the existence of the strange molecular partners of  $P_c$  states.

## ACKNOWLEDGMENTS

We thank useful discussions and valuable comments from Feng-Kun Guo and Jia-Jun Wu. This work is supported by the NSFC and the Deutsche Forschungsgemeinschaft (DFG, German Research Foundation) via the funds provided to the Sino-German Collaborative Research Center TRR110 Symmetries and the Emergence of Structure in QCD (NSFC Grant No. 12070131001, DFG Project-ID 196253076-TRR 110), by the NSFC Grants No. 11835015 and No. 12047503, and by the Chinese Academy of Sciences (CAS) under Grant No. XDB34030000.

## APPENDIX: $N^*$ HADRONIC MOLECULES

For the  $N^*(2270)$  as the  $K^*\Sigma^*$  molecular, it should be mentioned that the sets of spin and parity for  $(K^*, \Sigma^*)$  is  $(1^-, 3/2^+)$ . Thus the  $N^*$  states of spin-parity  $(1/2^-, 3/2^-, 5/2^-)$  may be considered as  $S$ -wave bound states of  $K^*\Sigma^*$ . Subject to the Lorentz covariant orbital-spin scheme, the  $S$ -wave couplings for the  $N^*$  with  $J^P = 1/2^-$  and  $3/2^-$  with the meson-baryon pairs of interest are given by

$$\mathcal{L}_{K^*\Sigma^*N^*(1/2^-)} = g_{K^*\Sigma^*N^*}^{1/2^-} \bar{\Sigma}_\mu^* N^* K^{*\mu}, \quad (\text{A1})$$

$$\mathcal{L}_{K^*\Sigma^*N^*(3/2^-)} = g_{K^*\Sigma^*N^*}^{3/2^-} \bar{\Sigma}^{*\mu} \gamma_5 \tilde{\gamma}^\nu N_\mu^* K_\nu^*, \quad (\text{A2})$$

where  $\tilde{\gamma}^\nu = (g_{\mu\nu} - \frac{p_\mu p_\nu}{p^2})\gamma^\mu$  with  $p_\mu$  representing the momentum of initial  $N^*$  state. And two  $S$ -wave coupling constants  $g_{K^*\Sigma^*N^*}^{1/2^-}$  and  $g_{K^*\Sigma^*N^*}^{3/2^-}$  can be estimated by the

TABLE III. The coupling constants used in our calculation.

$g_{KN\Sigma^*}$ ( $\text{GeV}^{-1}$ )	$g_{KN\Sigma}$ ( $\text{GeV}^{-1}$ )	$g_{K^*K\phi}$	$g_{K^*K^*\phi}$
6.202	8.444	9.077	4.271
$g_{KN\Sigma}$	$g_{K^*N\Sigma}$	$g_{K_0^*K_0\gamma}$ ( $\text{GeV}^{-1}$ )	$g_{K_c^*K_c\gamma}$ ( $\text{GeV}^{-1}$ )
2.7	-3.25	-0.385	0.253

Weinberg compositeness criterion [4,50,51]:

$$g_{K^*\Sigma^*N^*}^{1/2^-} = \sqrt{\frac{2\pi m_2 \sqrt{2\epsilon}}{\mu^{3/2}}}, \quad (\text{A3})$$

$$g_{K^*\Sigma^*N^*}^{3/2^-} = \sqrt{\frac{12\pi m_2 \sqrt{2\epsilon}}{5\mu^{3/2}}}, \quad (\text{A4})$$

where  $\mu = m_1 m_2 / (m_1 + m_2)$  is the reduced mass of the bound particles,  $m_1$  and  $m_2$  denote the masses of  $\Sigma^*$  and  $K^*$ , respectively, and  $\epsilon = m_1 + m_2 - M$  is the binding energy.

Similarly, for the  $N^*(2080)(3/2^-)$  as the  $K^*\Sigma$  molecular, the  $S$ -wave coupling can be written as

$$\mathcal{L}_{K^*\Sigma N^*(3/2^-)} = g_{K^*\Sigma N^*}^{3/2^-} \bar{\Sigma} N_\mu^* K^{*\mu}, \quad (\text{A5})$$

$$g_{K^*\Sigma N^*}^{3/2^-} = \sqrt{\frac{4\pi m_2 \sqrt{2\epsilon}}{\mu^{3/2}}}. \quad (\text{A6})$$

As shown in Fig. 8, we calculate the partial decay width of the molecular state by calculating this triangle diagram, the process considered in Table II. Therefore we also need the following effective Lagrangians [40]:

$$\mathcal{L}_{V_1 V_2 P} = -g_{V_1 V_2 P} \varepsilon^{\mu\nu\alpha\beta} (\partial_\mu V_{1\nu} \partial_\alpha V_{2\beta}) P,$$

$$\begin{aligned} \mathcal{L}_{V_1 V_2 V_3} = & -ig_{V_1 V_2 V_3} \{V_1^\mu (\partial_\mu V_2^\nu V_{3\nu} - V_2^\nu \partial_\mu V_{3\nu}) \\ & + (\partial_\mu V_{1\nu} V_2^\nu - V_{1\nu} \partial_\mu V_2^\nu) V_3^\mu \\ & + V_2^\mu (V_1^\nu \partial_\mu V_{3\nu} - \partial_\mu V_{1\nu} V_3^\nu)\}, \end{aligned}$$

$$\mathcal{L}_{PBB^*} = g_{PBB^*} \bar{B}^{*\mu} \partial_\mu P B,$$

$$\mathcal{L}_{VBB^*} = -ig_{VBB^*} \bar{B}^{*\mu} \gamma^\nu \gamma_5 [\partial_\mu V_\nu - \partial_\nu V_\mu] B,$$

$$\mathcal{L}_{PB_1 B_2} = -ig_{PB_1 B_2} \bar{B}_1 \gamma_5 B_2 P,$$

$$\mathcal{L}_{VB_1 B_2} = g_{PB_1 B_2} \bar{B}_1 \gamma_\mu V^\mu B_2,$$

where  $V_1 V_2 P$  denotes  $K^* K \phi$  or  $K^* K \gamma$ ,  $V_1 V_2 V_3$  denotes  $K^* K^* \phi$  or  $K^* K^* \gamma$ ,  $PBB^*$  denotes  $K p \Sigma^*$ ,  $VBB^*$  denotes  $K^* p \Sigma^*$ ,  $PB_1 B_2$  denotes  $K p \Sigma$ ,  $VB_1 B_2$  denotes  $K^* p \Sigma$ .

Here, we list the exact values of the coupling constants involved in our calculations in Table III, where  $g_{\gamma K^* K}$  is derived from the radiative decay of  $K^*$  in PDG [30], and the other constants are derived from the SU(3) flavor symmetry [52,53].

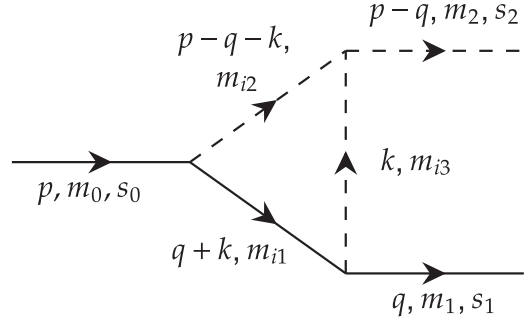


FIG. 9. The particle's momentums of the triangle diagram.

In order to make the calculation reasonable, we add two form factors. We adopt the following Gaussian regulator  $f_1$  to suppress short-distance contributions, and introduce the monopole form factor  $f_2$  to suppress the off-shell contributions for the exchanged particles:

$$f_1(\mathbf{p}^2 / \Lambda_0^2) = \exp(-\mathbf{p}^2 / \Lambda_0^2), \quad (\text{A7})$$

$$f_2(q^2) = \frac{\Lambda_1^4}{(m^2 - q^2)^2 + \Lambda_1^4}, \quad (\text{A8})$$

where  $\mathbf{p}$  is the spatial part of the momentum of  $K^*$  or  $\Sigma^*$  in the rest frame of the  $N^*$  state,  $m$  is the mass of the exchanged particle, and  $q$  is the corresponding momentum.  $\Lambda_0$  and  $\Lambda_1$  are ultraviolet cut-off and off-shell cutoff, respectively. The cutoff  $\Lambda_0$  denotes a hard momentum scale that suppresses the contribution of the two constituents at short distances  $\sim 1/\Lambda_0$ . There is no universal criterion for choosing the cut-off, but as a general rule, the value of  $\Lambda_0$  should be much larger than the typical momentum in the bound state, given by  $\sqrt{2\mu\epsilon}$ . It should also not be too large since we have neglected all other degrees of freedom, except for the two constituents, which would play a role at short distances. Here, we range  $\Lambda_0$  from 0.6 GeV to 1.4 GeV. The cut-off  $\Lambda_1$  for the off-shell form factor varies for the different systems, and we vary it in the range of 0.8 GeV to 2.0 GeV.

So, following the momentums notation in Fig. 9, the corresponding amplitude can be written as

$$\begin{aligned} \mathcal{M}_i = & g_0 g_1 g_2 \int_{-\infty}^{\infty} \frac{d^4 k}{(2\pi)^4} \exp\left\{-\frac{(\mathbf{q} + \mathbf{k})^2}{\Lambda_0^2}\right\} \frac{\Lambda_1^4}{(m_{i3}^2 - k^2)^2 + \Lambda_1^4} \\ & \times \frac{A_i(k)}{[(\mathbf{q} + \mathbf{k})^2 - m_{i1}^2 + i\epsilon_{i1}][(\mathbf{p} - \mathbf{q} - \mathbf{k})^2 - m_{i2}^2 + i\epsilon_{i2}](k^2 - m_{i3}^2 + i\epsilon_{i3})}, \end{aligned} \quad (\text{A9})$$

$$A_{N^*(2270),K}^{1/2} = \bar{u}(q, s_1) (\not{q} + \not{k} + m_{i1}) \mathcal{P}_{3/2^+}^{\mu\nu} (q + k, m_{i1}) u(p, s_0) k_\mu \tilde{g}_{\nu\sigma}^{i2} \varepsilon^{\lambda\sigma\alpha\beta} (p - q - k)_\lambda (p - q)_\alpha \varepsilon_\beta^*(p - q, s_2), \quad (\text{A10})$$

$$\begin{aligned} A_{N^*(2270),K^*}^{1/2} = & \bar{u}(q, s_1) \gamma_5 \gamma^\nu (\not{q} + \not{k} + m_{i1}) \mathcal{P}_{3/2^+}^{\mu\alpha} (q + k, m_{i1}) u(p, s_0) \{k_\mu (p - q + k)^\lambda \tilde{g}_{\alpha\lambda}^{i2} \tilde{g}_\nu^{i3\beta} \\ & + k_\mu (p - q - 2k)^\beta \tilde{g}_{\alpha\lambda}^{i2} \tilde{g}_\nu^{i3\lambda} + k_\mu (k - 2p + 2q)_\lambda \tilde{g}_\alpha^{i2\beta} \tilde{g}_\nu^{i3\lambda} - (\mu \leftrightarrow \nu)\} \varepsilon_\beta^*(p - q, s_2), \end{aligned} \quad (\text{A11})$$

$$A_{N^*(2270),K}^{3/2} = \bar{u}(q, s_1) (\not{q} + \not{k} + m_{i1}) \mathcal{P}_{3/2^+}^{\mu\nu} (q + k, m_{i1}) \gamma_5 \tilde{\gamma}^\rho u_\nu(p, s_0) k_\mu \tilde{g}_{\rho\sigma}^{i2} \varepsilon^{\lambda\sigma\alpha\beta} (p - q - k)_\lambda (p - q)_\alpha \varepsilon_\beta^*(p - q, s_2), \quad (\text{A12})$$

$$\begin{aligned} A_{N^*(2270),K^*}^{3/2} = & \bar{u}(q, s_1) \gamma_5 \gamma^\nu (\not{q} + \not{k} + m_{i1}) \mathcal{P}_{3/2^+}^{\mu\alpha} (q + k, m_{i1}) \gamma_5 \tilde{\gamma}^\beta u_\alpha(p, s_0) \{k_\mu (p - q + k)^\lambda \tilde{g}_{\beta\lambda}^{i2} \tilde{g}_\nu^{i3\sigma} \\ & + k_\mu (p - q - 2k)^\sigma \tilde{g}_{\beta\lambda}^{i2} \tilde{g}_\nu^{i3\lambda} + k_\mu (k - 2p + 2q)_\lambda \tilde{g}_\beta^{i2\sigma} \tilde{g}_\nu^{i3\lambda} - (\mu \leftrightarrow \nu)\} \varepsilon_\sigma^*(p - q, s_2), \end{aligned} \quad (\text{A13})$$

TABLE IV. The values of ( $|A_{3/2}/A_{1/2}|$ ,  $\Gamma_{\gamma p}$ ,  $\Gamma_{p\phi}$ ) at different cutoffs from the triangle diagram.

$(\Lambda_0, \Lambda_1)(\text{GeV})$		(0.6,0.8)	(0.8,1.1)	(1.0,1.4)	(1.2,1.7)	(1.4,2.0)
$N^*(2080)(3/2^-)$	$ A_{3/2}/A_{1/2} $	1.90	2.04	2.16	2.27	2.39
	$\Gamma_{\gamma p}(\text{KeV})$	0.047	0.28	0.69	1.16	1.64
	$\Gamma_{p\phi}(\text{MeV})$	2.34	14.97	41.09	78.70	127.98
$N^*(2270)(3/2^-)$	$ A_{3/2}/A_{1/2} $	1.06	1.12	1.19	1.26	1.32
	$\Gamma_{\gamma p}(\text{KeV})$	0.53	4.56	15.65	35.56	65.72
	$\Gamma_{p\phi}(\text{MeV})$	2.87	21.86	88.85	256.19	605.63

$$A_{N^*(2080),K}^{3/2} = \bar{u}(q, s_1) \gamma_5 (\not{q} + \not{k} + m_{i1}) u^\rho(p, s_0) \tilde{g}_{\nu\rho}^{i2} \epsilon^{\mu\nu\alpha\beta} (p - q - k)_\mu (p - q)_\alpha \epsilon_\beta^*(p - q, s_2), \quad (\text{A14})$$

$$\begin{aligned} A_{N^*(2080),K^*}^{3/2} = & \bar{u}(q, s_1) \gamma_\mu (\not{q} + \not{k} + m_{i1}) u_\nu(p, s_0) \{ (p - q + k)_\alpha \tilde{g}_{i2}^{\nu\alpha} \tilde{g}_{i3}^{\mu\beta} \\ & + (p - q - 2k)^\beta \tilde{g}_{i2\alpha}^\nu \tilde{g}_{i3}^{\mu\alpha} + (k - 2p + 2q)_\alpha \tilde{g}_{i2}^{\nu\beta} \tilde{g}_{i3}^{\mu\alpha} \} \epsilon_\beta^*(p - q, s_2) \\ = & \bar{u}(q, s_1) \gamma_\mu (\not{q} + \not{k} + m_{i1}) u_\nu(p, s_0) \tilde{g}_{i2}^{\nu\alpha} \tilde{g}_{i3}^{\mu\beta} \{ g_{\beta\lambda} (p - q + k)_\alpha \\ & + g_{\alpha\beta} (p - q - 2k)_\lambda + g_{\lambda\alpha} (k - 2p + 2q)_\beta \} \epsilon^{*\lambda}(p - q, s_2), \end{aligned} \quad (\text{A15})$$

where  $\epsilon_{i1} = m_{i1} \Gamma_{i1}$ ,  $\epsilon_{i2} = m_{i2} \Gamma_{i2}$ ,  $\epsilon_{i3} = m_{i3} \Gamma_{i3}$ , and  $\tilde{g}_{\mu\nu}^{i2} \equiv \tilde{g}_{\mu\nu}(p - q - k, m_{i2})$ ,  $\tilde{g}_{\mu\nu}^{i3} \equiv \tilde{g}_{\mu\nu}(k, m_{i3})$ ,  $\tilde{g}_{\mu\nu}(p, m) = g_{\mu\nu} - p_\mu p_\nu / m^2$ .

$A_{N^*(2270);K,K^*}^{1/2,3/2}$  or  $A_{N^*(2080);K,K^*}^{3/2}$  correspond to the  $p\gamma$  or  $p\phi$  channel with  $K, K^*$  exchange of triangle diagrams for two-body decays of the  $N^*(2270)(1/2^-)$ ,  $N^*(2270)(3/2^-)$  or  $N^*(2080)(3/2^-)$ .

So, we can calculate the squared amplitude and width by

$$|\mathcal{M}|^2 = |\mathcal{M}_K|^2 + |\mathcal{M}_{K^*}|^2, \quad (\text{A16})$$

$$d\Gamma = \frac{1}{32\pi^2} \frac{|\mathcal{M}|^2}{2J+1} \frac{|\vec{q}|}{m_0^2} d\Omega. \quad (\text{A17})$$

Then we list the corresponding results in Table IV.

- 
- [1] R. Aaij *et al.* (LHCb Collaboration), *Phys. Rev. Lett.* **115**, 072001 (2015).  
[2] R. Aaij *et al.* (LHCb Collaboration), *Phys. Rev. Lett.* **122**, 222001 (2019).  
[3] H. X. Chen, W. Chen, X. Liu, and S. L. Zhu, *Phys. Rep.* **639**, 1 (2016).  
[4] F. K. Guo, C. Hanhart, Ulf-G. Meißner, Q. Wang, Q. Zhao, and B. S. Zou, *Rev. Mod. Phys.* **90**, 015004 (2018); **94**, 029901(E) (2022).  
[5] Y. R. Liu, H. X. Chen, W. Chen, X. Liu, and S. L. Zhu, *Prog. Part. Nucl. Phys.* **107**, 237 (2019).  
[6] J. J. Wu, R. Molina, E. Oset, and B. S. Zou, *Phys. Rev. Lett.* **105**, 232001 (2010).  
[7] J. J. Wu, R. Molina, E. Oset, and B. S. Zou, *Phys. Rev. C* **84**, 015202 (2011).  
[8] W. L. Wang, F. Huang, Z. Y. Zhang, and B. S. Zou, *Phys. Rev. C* **84**, 015203 (2011).  
[9] J. J. Wu, T. S. H. Lee, and B. S. Zou, *Phys. Rev. C* **100**, 035206 (2019).  
[10] C. W. Xiao, J. Nieves, and E. Oset, *Phys. Rev. D* **88**, 056012 (2013).  
[11] M. Z. Liu, Y. W. Pan, F. Z. Peng, M. S. Sánchez, L. S. Geng, A. Hosaka, and M. P. Valderrama, *Phys. Rev. Lett.* **122**, 242001 (2019).  
[12] M. L. Du, V. Baru, F. K. Guo, C. Hanhart, Ulf-G. Meißner, J. A. Oller, and Q. Wang, *Phys. Rev. Lett.* **124**, 072001 (2020).  
[13] J. He, *Phys. Rev. D* **95**, 074031 (2017).  
[14] B. Zou and J. Dai, *Nucl. Phys. Rev.* **35**, 369 (2018).  
[15] Y. H. Lin, C. W. Shen, and B. S. Zou, *Nucl. Phys. A* **980**, 21 (2018).  
[16] D. Ben, A. C. Wang, F. Huang, and B. S. Zou, *arXiv:2302.14308*.  
[17] B. Dey *et al.* (CLAS Collaboration), *Phys. Rev. C* **89**, 055208 (2014).  
[18] H. Seraydaryan *et al.* (CLAS Collaboration), *Phys. Rev. C* **89**, 055206 (2014).  
[19] Q. Zhao, J. P. Didelez, M. Guidal, and B. Saghai, *Nucl. Phys. A* **660**, 323 (1999).  
[20] A. I. Titov, T. S. H. Lee, H. Toki, and O. Streltsova, *Phys. Rev. C* **60**, 035205 (1999).  
[21] Y. S. Oh and H. C. Bhang, *Phys. Rev. C* **64**, 055207 (2001).  
[22] Q. Zhao, B. Saghai, and J. S. Al-Khalili, *Phys. Lett. B* **509**, 231 (2001).  
[23] A. I. Titov and B. Kampfer, *Phys. Rev. C* **76**, 035202 (2007).  
[24] S. Ozaki, A. Hosaka, H. Nagahiro, and O. Scholten, *Phys. Rev. C* **80**, 035201 (2009); **81**, 059901(E) (2010).  
[25] A. Kiswandhi, J. J. Xie, and S. N. Yang, *Phys. Lett. B* **691**, 214 (2010).

- [26] H. Y. Ryu, A. I. Titov, A. Hosaka, and H. C. Kim, *Prog. Theor. Exp. Phys.* (2014) 023D03.
- [27] B. G. Yu, H. Kim, and K. J. Kong, *Phys. Rev. D* **95**, 014020 (2017).
- [28] S. H. Kim and S. I. Nam, *Phys. Rev. C* **100**, 065208 (2019).
- [29] S. H. Kim and S. I. Nam, *Phys. Rev. C* **101**, 065201 (2020).
- [30] R. L. Workman *et al.* (Particle Data Group), *Prog. Theor. Exp. Phys.* (2022) 083C01.
- [31] S. H. Kim, T. S. H. Lee, S. I. Nam, and Y. Oh, *Phys. Rev. C* **104**, 045202 (2021).
- [32] A. Donnachie and P. V. Landshoff, *Nucl. Phys. B* **244**, 322 (1984).
- [33] J. M. Laget and R. Mendez-Galain, *Nucl. Phys. A* **581**, 397 (1995).
- [34] M. A. Pichowsky and T. S. H. Lee, *Phys. Rev. D* **56**, 1644 (1997).
- [35] Y. S. Oh, A. I. Titov, and T. S. H. Lee, *Phys. Rev. C* **63**, 025201 (2001).
- [36] M. Birkel and H. Fritzsche, *Phys. Rev. D* **53**, 6195 (1996).
- [37] M. J. Yan, F. Z. Peng, M. Sánchez Sánchez, and M. Pavon Valderrama, *Phys. Rev. D* **104**, 114025 (2021).
- [38] V. G. J. Stoks and T. A. Rijken, *Phys. Rev. C* **59**, 3009 (1999).
- [39] T. A. Rijken, V. G. J. Stoks, and Y. Yamamoto, *Phys. Rev. C* **59**, 21 (1999).
- [40] Y. H. Lin, C. W. Shen, F. K. Guo, and B. S. Zou, *Phys. Rev. D* **95**, 114017 (2017).
- [41] C. W. Shen, F. K. Guo, J. J. Xie, and B. S. Zou, *Nucl. Phys. A* **954**, 393 (2016).
- [42] Y. Oh, C. M. Ko, and K. Nakayama, *Phys. Rev. C* **77**, 045204 (2008).
- [43] F. James and M. Roos, *Comput. Phys. Commun.* **10**, 343 (1975).
- [44] H. Dembinski *et al.* (iminuit team), iminuit: A Python interface to MINUIT, <https://github.com/scikit-hep/iminuit>.
- [45] F.-K. Guo, IMinuit.jl: A Julia wrapper of iminuit, <https://github.com/fkguo/IMinuit.jl>.
- [46] J. Ballam, G. B. Chadwick, Y. Eisenberg, E. Kogan, K. C. Moffeit, P. Seyboth, I. O. Skillicorn, H. Spitzer, G. E. Wolf, H. H. Bingham *et al.*, *Phys. Rev. D* **7**, 3150 (1973).
- [47] R. M. Egloff, P. J. Davis, G. Luste, J. F. Martin, J. D. Prentice, D. O. Caldwell, J. P. Cumalat, A. M. Eisner, A. Lu, R. J. Morrison *et al.*, *Phys. Rev. Lett.* **43**, 657 (1979).
- [48] D. P. Barber, J. B. Dainton, L. C. Y. Lee, R. Marshall, J. C. Thompson, D. T. Williams, T. J. Brodbeck, G. Frost, G. N. Patrick, G. F. Pearce *et al.*, *Z. Phys. C* **12**, 1 (1982).
- [49] J. Busenitz, C. Olszewski, P. Callahan, G. Gladding, A. Wattenberg, M. E. Binkley, J. Butler, J. P. Cumalat, I. Gaines, M. Gormley *et al.*, *Phys. Rev. D* **40**, 1 (1989).
- [50] S. Weinberg, *Phys. Rev.* **137**, B672 (1965).
- [51] V. Baru, J. Haidenbauer, C. Hanhart, Y. Kalashnikova, and A. E. Kudryavtsev, *Phys. Lett. B* **586**, 53 (2004).
- [52] J. J. de Swart, *Rev. Mod. Phys.* **35**, 916 (1963); **37**, 326 (1965).
- [53] D. Rönchen, M. Doring, F. Huang, H. Haberzettl, J. Haidenbauer, C. Hanhart, S. Krewald, U. G. Meissner, and K. Nakayama, *Eur. Phys. J. A* **49**, 44 (2013).